Report of the National Research Center for Disaster Prevention, No. 44, October. 1989

511. 501.7 : 551. 515. 4 : 578. 45

# The Doppler Radar of NRCDP and Observations of Meso-Scale Weather Systems

by

**Masayuki Maki*, Tsuruhei Yagi* and Sento Nakai***

*National Research Center for Disaster Prevention, Japan*

**Abstract**

The Doppler radar of the National Research Center for Disaster Prevention was completed in March, 1988. The main characteristics of the radar are (1) an antenna with rapid scanning abilities, (2) various antenna scan modes computer-controlled, (3) a real time color display of rainfall intensity, Doppler velocity and Doppler spectrum width, and (4) portability. NRCDP's Doppler radar is useful to study three-dimensional structures of meso-scale severe weather phenomena. Several examples of the Doppler radar observations are shown : stratiform precipitation in the Baiu season, a thunderstorm whose lifetime was so short that it could not be detected by the existing weather observation systems, a snowstorm associated with a monsoon burst in winter, and an orographically induced or enhanced snowfall in the inland area of the Tohoku District. The antenna scanning modes appropriate for three-dimensional observations of these phenomena are also discussed herein.

**Key words :** Dappler radar, meso-scale, thunderstorm, snow storn

## 1. Introduction

Various weather phenomena which we experience every day may be grouped into several classes according to their typical horizontal scales and lifetimes, as shown in Fig. 1. Some of these weather phenomena are disastrous and often do serious damage to the public property and our daily lives (Oyagi *et al.*, 1984 ; Kinosita *et al.*, 1987 ; Tanaka *et al.*, 1988). To predict the occurrence of meteorological disasters it is essential to recognize the horizontal scale and lifetime of the weather systems and select adequate observation methods and instruments.

At present, there are various types of weather observation systems in Japan. For example, the Japan Meteorological Agency (JMA) has 18 upper air observation stations which measure the atmospheric pressure, air temperature and humidity every 12 hours as well as the wind speed and wind direction every 6 hours. JMA also has a distribution of 20 stations of conventional weather radars and about 1300 AMeDAS (Automated

---

* Atmospheric Disaster Laboratory, First Research Division

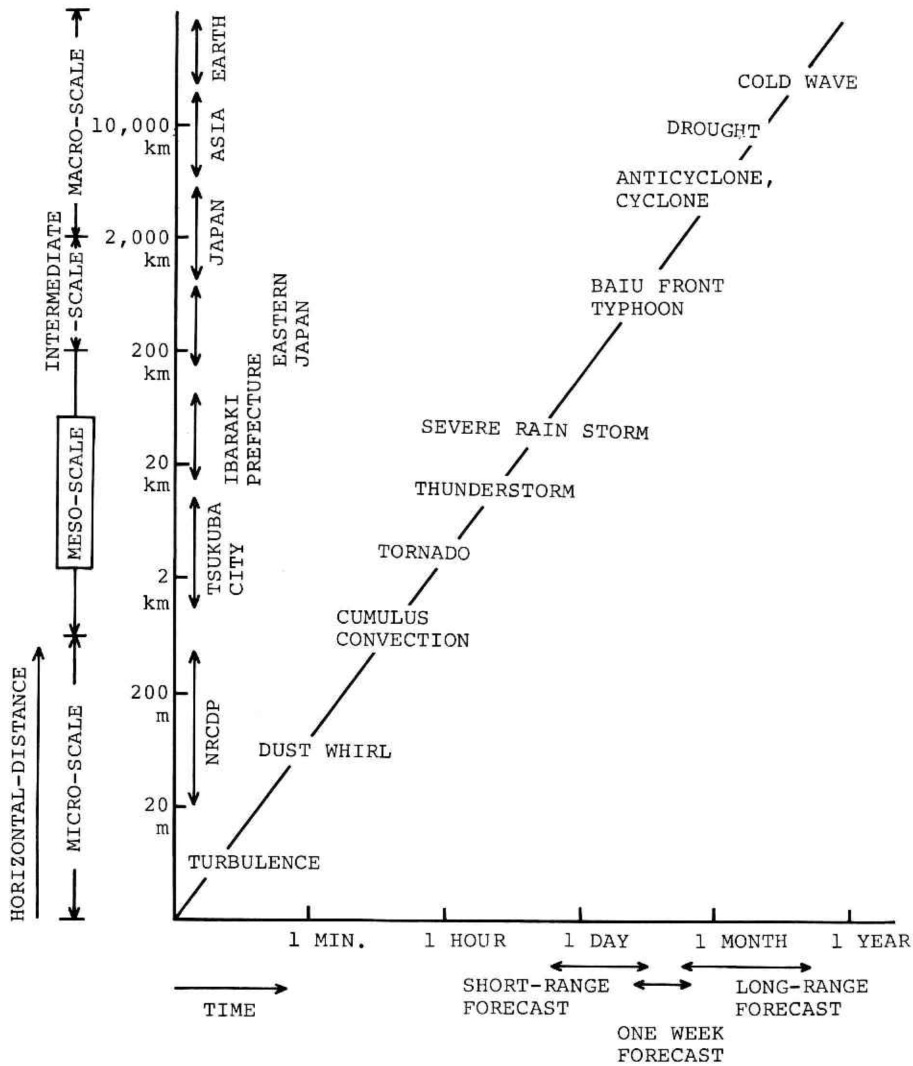


**Fig. 1** Horizontal scale and lifetime of various weather phenomena.

Meteorological Data Acquisition System) stations throughout Japan. Meteorological elements near the surface are measured at AMeDAS stations and the collected data are sent to the computer center of JMA through the public telephone lines. The radar-AMeDAS composite weather map can be seen daily on TV programs throughout Japan. In addition, cloud pictures over Japan provided by the GMS (Geostationary Meteorological Satellite) which is a part of the global satellite system in the world, can be seen. Although some attempts are made to forecast meso-scale weather using some of the weather observation systems mentioned above (Browning, 1982), there is no established method or system for forecasting the meso-scale phenomena yet. The reason is because the existing weather observation systems are designed mainly for short-range (about 2 days), one week, and long-range (about 6 months) forecasts. Also the systems are useful to forecast intermediate-scale weather phenomena such as anticyclones, cyclones, as well as typhoons and macro-scale weather phenomena. On the other hand, meso-scale phenomena such as severe rain storms, thunderstorms, and tornadoes are often overlooked in the present weather observation systems because of their small horizontal scale (from about a few hundred meters to several hundred kilometers) and their short lifetimes (from a few ten minutes to a day).

To overcome these difficulties and to study meso-scale severe weather phenomena which cause disasters, the use of the Doppler weather radar was proposed. The Doppler radar can detect the presence of disturbances, determine their direction and range, and clarify their three-dimensional structure in a few minutes. It can also measure the wind field in a disturbance using the Doppler effect. Recent applications of the Doppler radar for storm observations were reviewed by Uyeda (1986).

Several kinds of Doppler radars are used in the field of meteorology in Japan: a 5-cm wavelength Doppler radar of the Meteorological Research Institute (MRI) for observations of typhoons and cyclones; a 3-cm wavelength portable Doppler radar of MRI for severe rainfall observations; a three-dimensional scanning Doppler radar of the Institute of Low Temperature Science of Hokkaido University for studies of cloud physics; and a dual polarization Doppler radar of the Public Works Research Institute. In this paper, the main characteristics and the performance of NRCDP's Doppler weather radar which was completed in March, 1988 are described, and some examples of Doppler radar observations are shown. Suitable antenna scan modes for Doppler radar observations of meso-scale weather phenomena are also discussed.

## 2. Performance of the Doppler radar of National Research Center for Disaster Prevention (NRCDP)

NRCDP's Doppler weather radar was designed to study meso-scale severe weather phenomena such as snowstorms, local severe rain, thunderstorms, strong wind, and other local terrain-induced phenomena. The main characteristics of the radar are:

1) various antenna scan modes controlled by a computer;
2) high antenna rotation speed (max. 15rpm.);

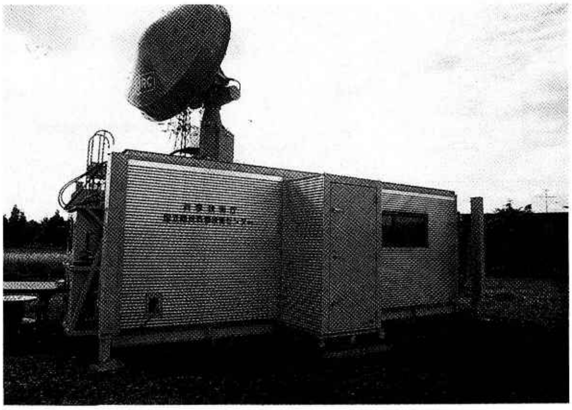

**Fig. 2** Exterior of NRCDP's Doppler radar.

3) real time color display of rainfall intensity, Doppler velocity, and Doppler spectrum width ;
4) portability.

The exterior of the radar and the interior of the radar shelter are shown in Fig. 2 and Fig. 3, respectively.

NRCDP's radar consists of several units as shown in Fig. 4. The teansmitter produces power at the radar frequency of 9415 MHz, which is modulated in the form of pulses of radio waves of 0.5 $\mu$sec and sent to the antenna at a "pulse-repetition

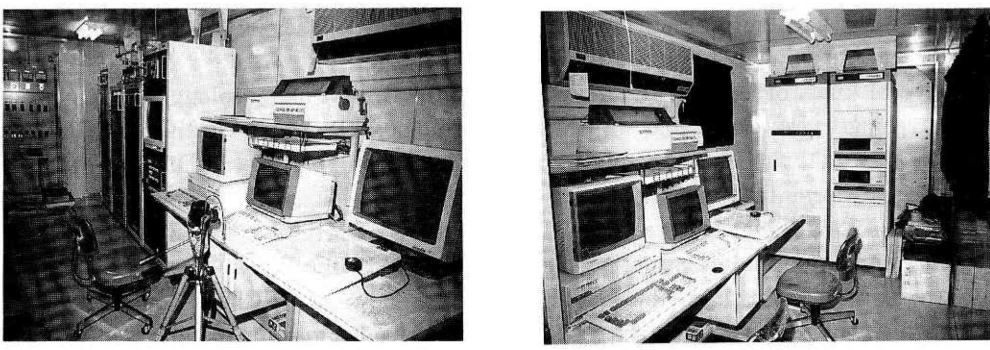

**Fig. 4** Constituents of NRCDP's Doppler radar.

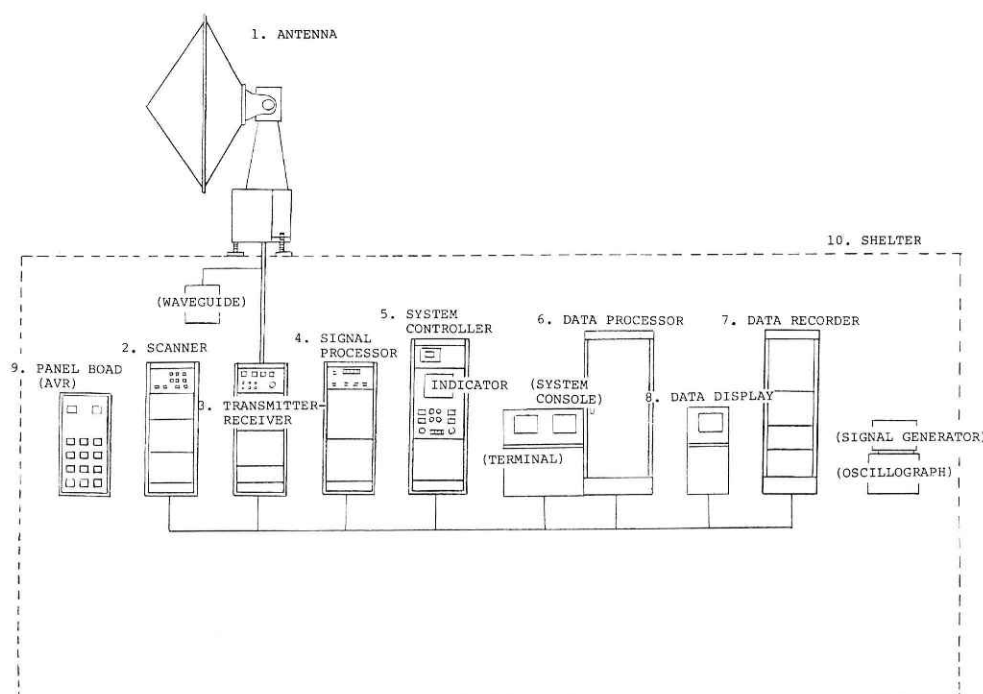


**Fig. 3** Interior of NRCDP's Doppler radar.

frequency" of 2000 Hz. The transmitted peak power is 40 kW. The antenna, which is a parabolic-shaped reflector and 2 m in diameter radiates this pulse-shaped power through the air in the form of a sharp pencil beam of 1.2 degrees in width. These values of radar specifications, which were determined by the radar equation, were selected

**Table 1** Specifications of NRCOP's Doppler radar

| | |
|---|---|
| 1. Antenna Assembly | |
| Reflector | 2 m aperture, circular parabola |
| Beam-width | 1.2° or less in horizontal and vertical |
| Gain | 42 dB |
| Polarization | Horizontal |
| 2. Scanner | |
| Azimuth angle | 360° around |
| Elevation angle | −5°～185° |
| Scan rate | 15 rpm (max.) |
| Scan control | Manual-mode<br>CPU-mode : PPI, RHI, CAPPI, SPPI, SRHI<br>Program-mode (Combination of CPU-modes) |
| 3. Transmitter-Receiver | |
| Transmitter Aspect | |
| Radar frequency | 9, 415 MHz |
| Transmitted peak power | 40 kW |
| Transmitted pulse-width | 0.5 $\mu$sec |
| PRF | 2, 000 Hz |
| Transmitting tube | Magnetron |
| Receiver Aspect | |
| Noise figure | ≦ 5 dB |
| Minimum detectable signal | ≦ −110 dBm |
| Intermediate frequency | 30 MHz |
| Bandwidth | 2.0 MHz ± 0.5 MHz |
| 4. Signal Processor | |
| Reflectivity Mode | |
| Range correction | Subtraction method |
| Ground clutter elimination | MTI method |
| Averaging | Weighted moving average |
| Detectable intensity | 0.1 mm/h～100 mm/h |
| Range | 64 km |
| Doppler Mode | |
| Method | Pulse pair processing |
| Processed data | Doppler velocity, spectrum width |
| Velocity range | ± 16 m/sec |
| Resolution | 12.5 cm/sec |
| Range | 64 km |

5. System Controller and Indicator

| | |
|---|---|
| Control panel | Power supply control<br>Transmitter control<br>Antenna scan control (manual) |
| Indicator | 20-inch type CRT, 7 colors<br>A-Scope, 3 channels<br>PPI, RHI (Intensity, Doppler velocity, Spectrum width) |

6. Data Processor

| | |
|---|---|
| Computer | JAC 150, 32-bit<br>Max. memory capacity, 16 MB<br>Cycle time, 500 nsec or less<br>Computing speed, 1.25 $\mu$sec or less |
| System console | 14-inch type CRT, character (ASCII) |
| Terminal | Microcomputer |
| Software | Application program scheduler<br>Radar system control<br>Data collection and playback<br>Image data processing |

7. Data Recorder

| | |
|---|---|
| Magnetic disc unit | Memory capacity, 60 MB<br>Transfer rate, 806kB/sec or less |
| Floppy disc unit | 8-inch, 2 DD, 1 MB<br>Transfer rate, 2 MB/sec (read) |
| Magnetic tape unit | Transport, 2<br>Record density, 1600/6250 BPI<br>Tape speed, 100 IPS or more<br>9 track, 2400 feet, 1/2 inch |

8. Data Visual Display

| | |
|---|---|
| CRT | 20-inch type, high resolution<br>Zooming, Scrolling |
| Image memory | $2048\times1024\times4$ |
| Color | RGB, 16/4096 color |

9. Panel Boad

Automated voltage regulator (AVR)

| | |
|---|---|
| Input voltage | AC 200V (three phase) |
| Output voltage | AC 100V (single phase) |
| Consumption power | 10 kVA (max.) |

10. Shelter

Aluminum, Air-conditioned
Portable

under the constraints of portability and observations of meso-scale weather phenomena. A portion of this radiated power is intercepted and re-radiated in all directions by "targets" which are reflecting objects such as rain drops and snowflakes. The antenna collects the returned weak energy and delivers it to the receiver, where it is detected,

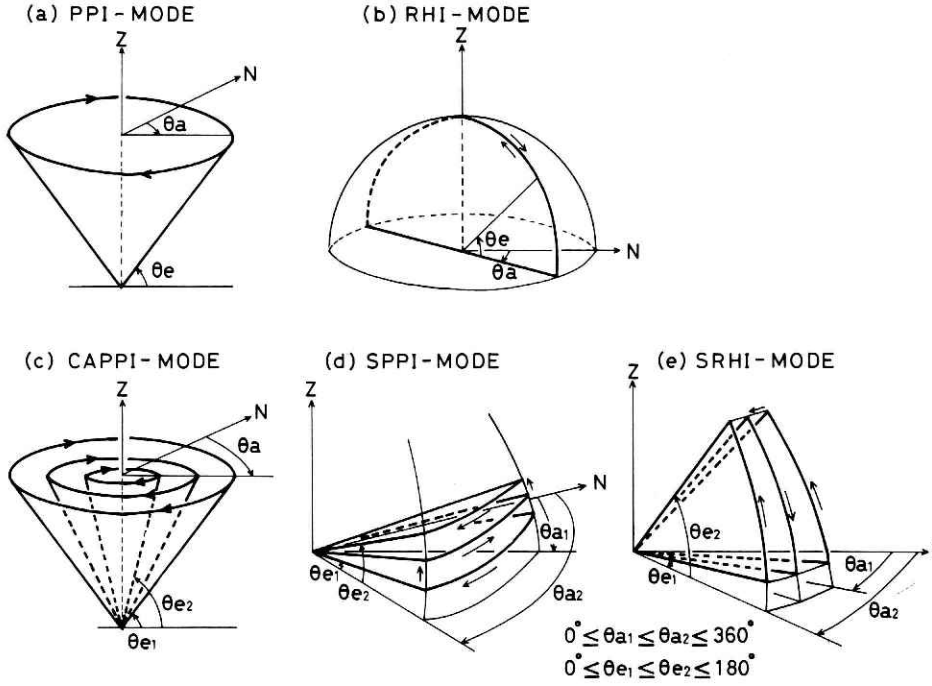


**Fig. 5** Schematic pictures of various antenna scan modes. PPI: Plan position indicator; RHI: Range height indicator; CAPPI: Constant altitude PPI; SPPI: Sector PPI; SRHI: Sector RHI.

amplified, and transformed into video form. This video signal is processed to detect the presence of the target and to extract its location and relative velocity. The processed data are recorded on the magnetic tape of the data recorder while they are indicated on the color display at real-time. More detailed specifications of the radar are shown in Table 1.

Among the characteristics of the radar mentioned previously, the most unique is the computer control of the antenna movement. The antenna is moved mechanically to scan the beam with various modes shown in Fig. 5. In the PPI (Plan-Position Indicator ) scan mode, the beam revolves around a vertical axis at any constant elevation angle, $\theta_e$. In the RHI (Range-Height Indicator) scan mode, the beam scans in an elevation at any constant azimuth angle, $\theta_a$. The CAPPI (Constant-Altitude Plan-Position Indicator) scan mode is a set of PPI scans and used to obtain the three-dimensional data of the weather phenomena. The SPPI (Sector-PPI) scan is a modification of the PPI scan in which the beam scan is restricted within the limits of any azimuth angle. The SRHI (Sector-RHI) scan is also a modification of the RHI scan in which the beam scan is restricted within the limits of any elevation angle. These antenna scan modes are also useful in observing the three-dimensional structre of meso-scale weather phenomena. A more detailed

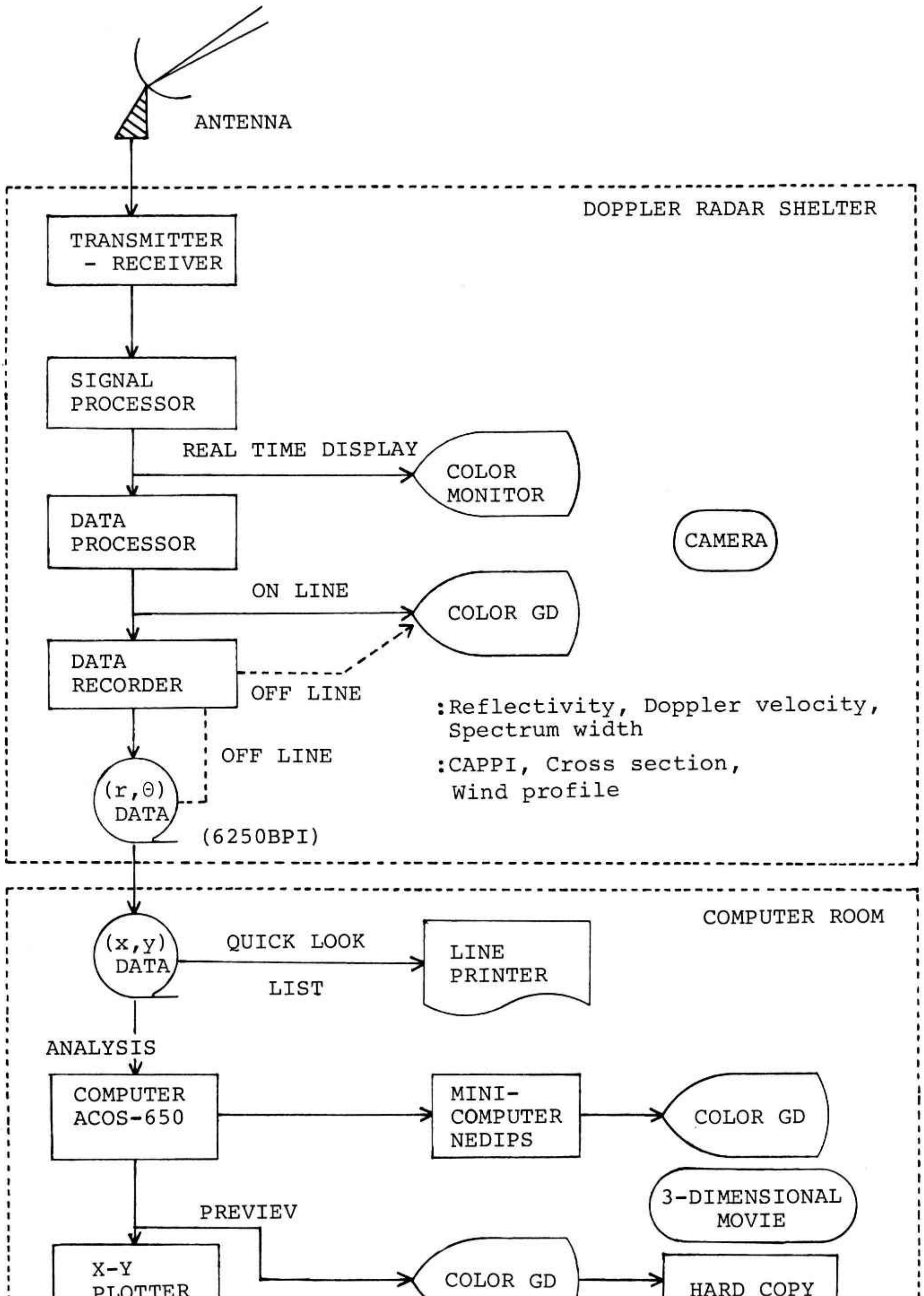


**Fig. 6** Flow of data and data analysis procedure.

discussion about the optimum scan mode for the three-dimensional observation will follow later.

The radar has another unique characteristic, rapid scanning of the antenna. The maximun antenna rotation speed is 15 rpm. This performance is also required for meso-scale weather observations. A detailed discussion regarding its effect on the signal processing was completed by Maki (1989).

As the collected data are extensive, skillful analyses of the data including data transformation and data file management are required. The flow of data and the procedure of data analyses are shown in Fig. 6. The process of data analyses are grouped into two stages : The first process is the basic analysis in the radar shelter and the second is the advanced analysis in the computer room of NRCDP. The radar reflectivity factor, Doppler velocity and Doppler spectrum width which are processed by the signal processor, are sent to the data processor and recorded on magnetic tapes in 6250 BPI. The data collected on magnetic tapes are analyzed by a 32-bit minicomputer (JAC-150) in the radar shelter and various kinds of image data are reproduced on the color graphic display. Basic structures of the observed weather phenomena are inferred from pictures shch as PPI, RHI, CAPPI images and time-height cross sections of the radar reflectivity factor and Doppler velocity. In addition to this, collected data can be also analyzed quantitatively by the general purpose computer, ACOS-650, when a more advanced analysis of the data or long calculation time is required. A three-dimensional display of the collected data and an echo picture which changes every second are made in the computer room.

## 3. Examples of weather phenomena observed with the Doppler radar

Some examples of weather phenomena observed with NRCDP's Doppler radar are shown in this section. The first example is stratiform precipitation observed during the Baiu season and the second is a thunderstorm observed in summer, whose scale and lifetime were so small that it could not be detected by the existing weather observation system such as AMeDAS of JMA. In both observations, the Doppler radar was located at NRCDP in Tsukuba City of Ibaraki Prefecture. The third example is a band-shaped snowfall accompanied by strong winds observed in the Tsugaru plain in the Tohoku District of Japan, which is associated with a monsoon burst over the Japan Sea in winter. The last example is an orographically induced or enhanced snowfall observed in the Shinjo basin which is also located in the Tohoku District.

### *STRATIFORM PRECIPITATION*

Weak rain from a thick stratiform cloud was observed on May 12, 1988 by NRCDP's Doppler radar. Fig. 7(a) is the real-time PPI display of the reflectivity obtained from a 360 degree scanning with the elevation angle of 10.5 degrees. The concentric circles show each 5 km radius from the radar site. The levels of reflectivity intensity 1, 2, 3, 4, 5, 6 correspond to the rainfall intensity of 0.1, 0.2, 0.7, 3, 12, 50 mm/hr respectively, when the empirical $Z$-$R$ relationship, $Z=200R^{1.6}$, is used ; where $Z$ it the reflectivity factor and $R$ the rainfall intensity. The concetric circular pattern of the radar echo in Fig. 7(a) represents the multi-layered structure of the precipitation system. This is seen more

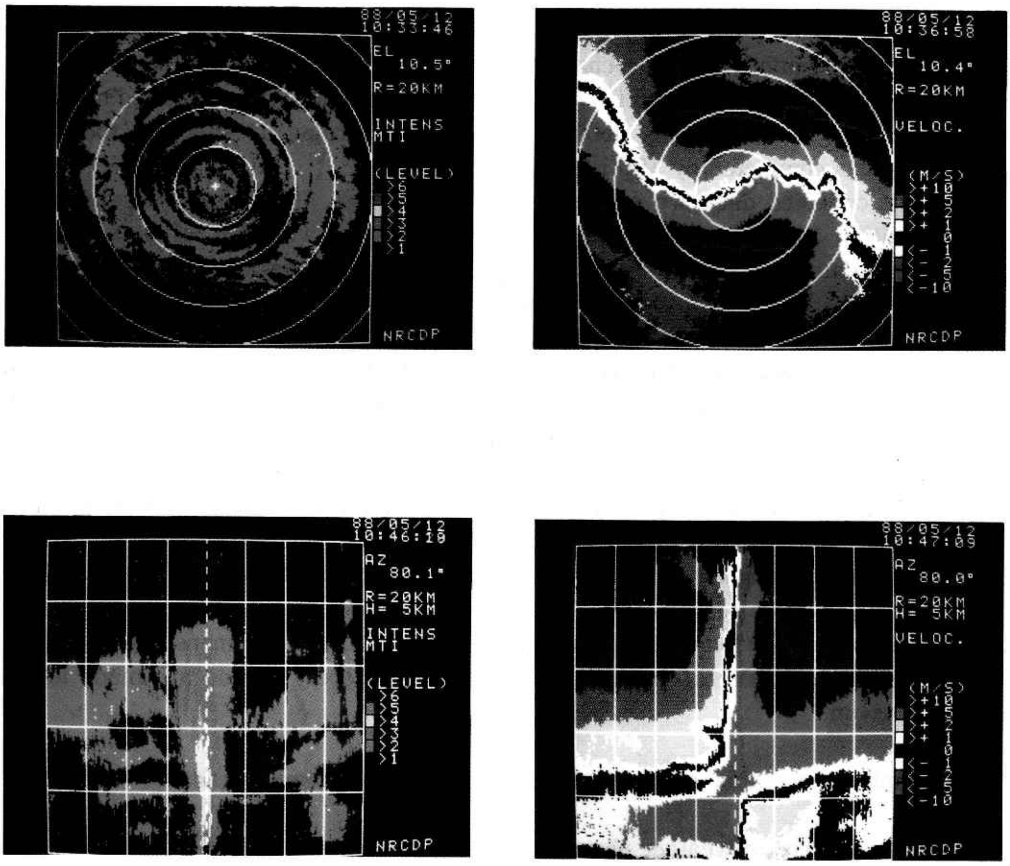


**Fig. 7** PPI display of (a) the reflectivity factor, (b) Doppler velocities, and RHI display of (c) the reflectivity factor, (d) Doppler velocities for stratiform precipitation of May 12, 1988.

clearly in the RHI display. Fig. 7(a) shows a vertical cross section of the reflectivity, the azimuth of which is 80. 1 degrees. The horizontal and vertical grid interval is 5 and 1km, respectively, and the radar location is at the center of the base. From Fig. 7(c), it is clear that 4 weak precipitating layers existed and that the echo top of the highest layer was about 4 km.

If relative motion exists between a target and the radar, the carrier frequency of the reflected wave is shifted, i.e., Doppler velocities can be observed. A PPI display of Doppler velocities at the same elevation angle as in Fig.7 (a) is shown in Fig. 7(b) and a RHI display of Doppler velocities in the same vertical cross section as in Fig. 7(c) is shown in Fig. 7(d). Interpretation of the Doppler velocity field requires experienced knowledge because a single Doppler radar maps a field of velocities that are directed

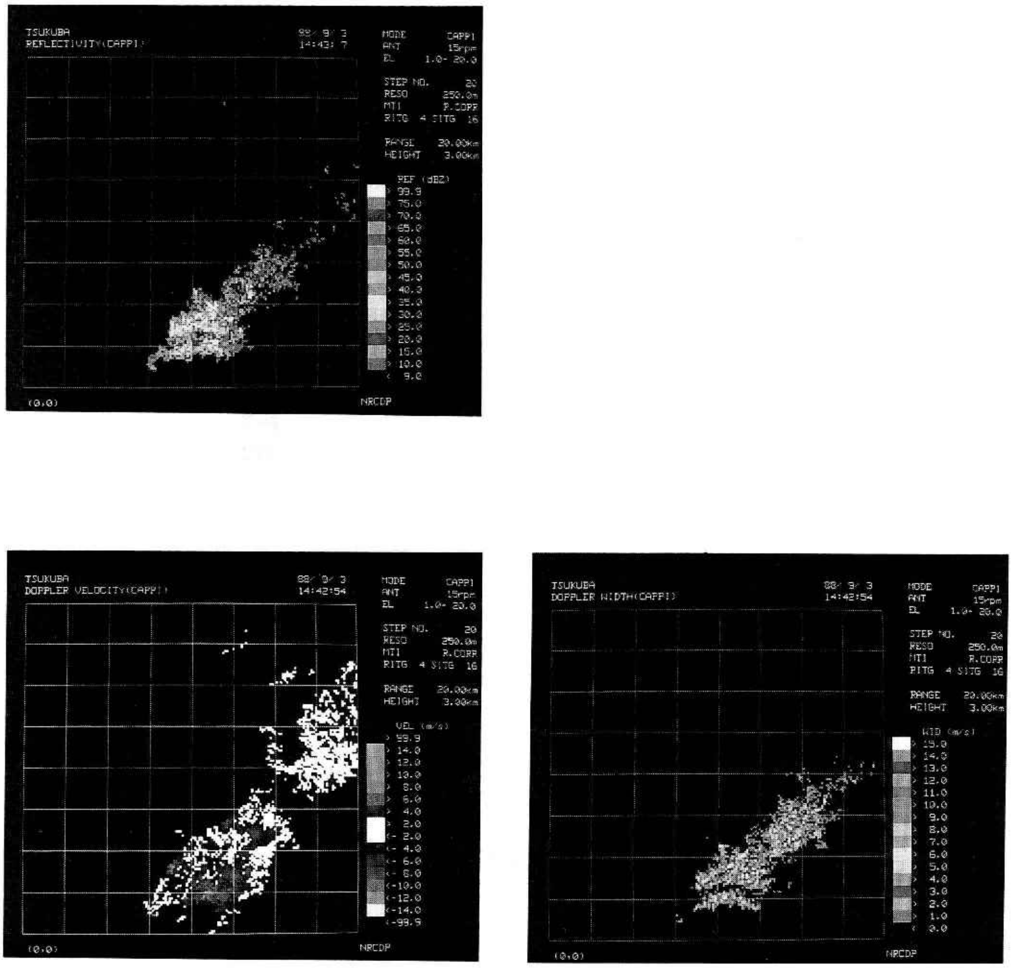


**Fig. 8** CAPPI display of (a) the reflectivity factor, (b) Doppler velocities, and (c) the spectrum width for the thunderstorm of September 3, 1988.

either toward or away from the radar site. However, several major features in the wind field can be drawn from a Doppler velocity pattern (Vincent and Brown, 1985). The zero velocity band bisecting the velocity field in Fig. 7(b) is S-shaped within about a 20 km range and the direction of the band changes from northwest to west at about the 20 km range (a height of 4 km). Because the wind direction at the zero velocity point is normal to the radar, this means that a southeast wind near the surface veers with a height up to about 4 km (20 km range) and then back above. The RHI image of the Doppler velocities (Fig. 7(d)) also confirms the above mentioned wind field.

*THUNDERSTORM*

A thunderstorm which could not be detected by the existing surface observation network was observed by NRCDP's Doppler radar on September 3, 1988. Unfortunately,

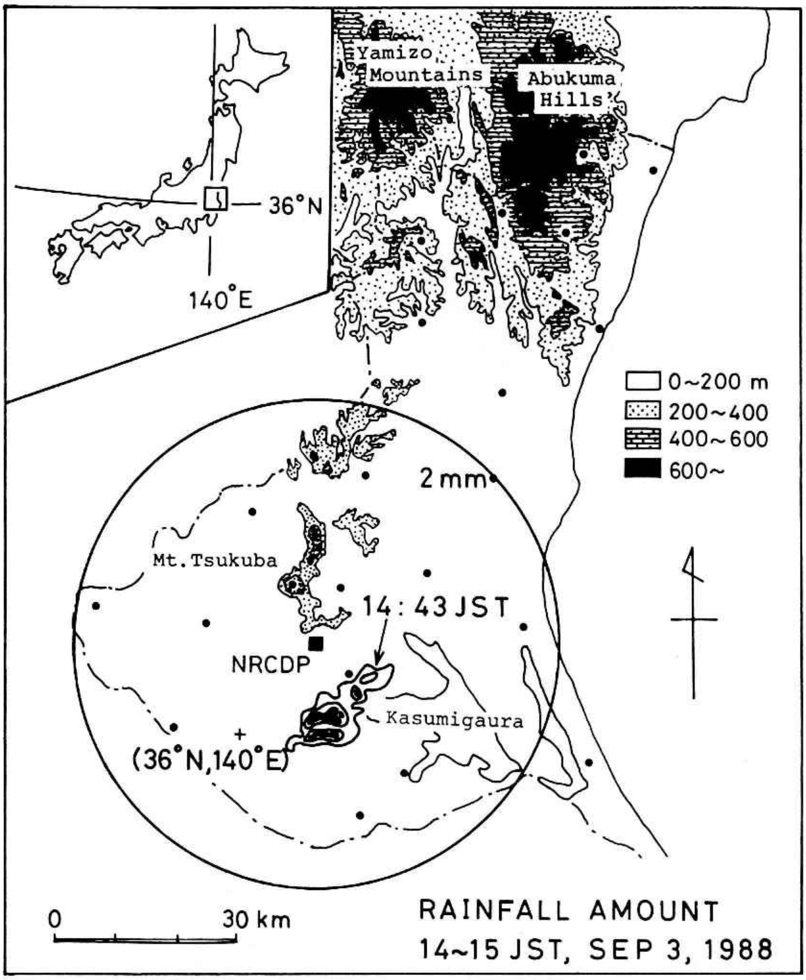


**Fig. 9** Composite map showing the location of a thunderstorm and the rainfall amount at the surface measured by AMeDAS. Topography and the radar observation area are also shown. Contour lines of the thunderstorm at 14 : 43 JST are drawn at 10 dBZ intervals and the black part shows the area whose intensity is larger than 30 dBZ.

as the observation was carried out during the test operating period of the radar, the whole stage of the thunderstorm development could not be observed. However, a three-dimensional observation was conducted at 14 : 30, 14 : 43 and 15 : 01 JST, respectively, and the following example shows the effectiveness of the NRCDP's rapid scan Doppler radar for local severe weather phenomena.

Fig. 8(a) is the CAPPI image of the reflectivity factor for the thunderstom, which is indicated on the high resolution color display. The height of the CAPPI is 3 km and the grid interval is 5 km. The location of the radar is at the center of the picture. In contrast to the first example, the reflectivity of the thunderstorm is 50 dBZ or more. This value corresponds to a rainfall intensity of 50 mm/h. Another typical characteristic of the thunderstorm is sharp gradients of intensity. Fig. 8(b) is a CAPPI display of Doppler velocities. It is difficult to estimate the wind field from the figure because a zero Doppler velocity band is not distinct in this case. Fig. 8(c) is a CAPPI display of the spectrum width which is an indicator of turbulence or a large wind shear. It is evident that a large wind shear zone exists in the thunderstorm and that it corresponds to a large reflectivity part of the storm.

It was inferred from the Doppler radar observation and the surface rain gauge data of AMeDAS (Fig. 9) that this thunderstorm occurred and developed rapidly after 14 JST. The storm stagnated at the same place about 15 km south to the radar site and it became extinct after 15 JST. According to Fig. 9, the size of the storm was so small that it could not be detected by the surface rain gauge measurements by AMeDAS.

*SNOWSTORM*

One of the disastrous meteorological phenomena in the northern part of Japan is a snowstorm accompanied with strong wind which can be a major obstacle for traffics and cause serious damage to the environment. The Shinjo branch of NRCDP has been studying snowstorms from the standpoint of glaciology (Sato and Higashiura, 1989), but the observation has been restricted in the surface boundary layer which is about 10 m in

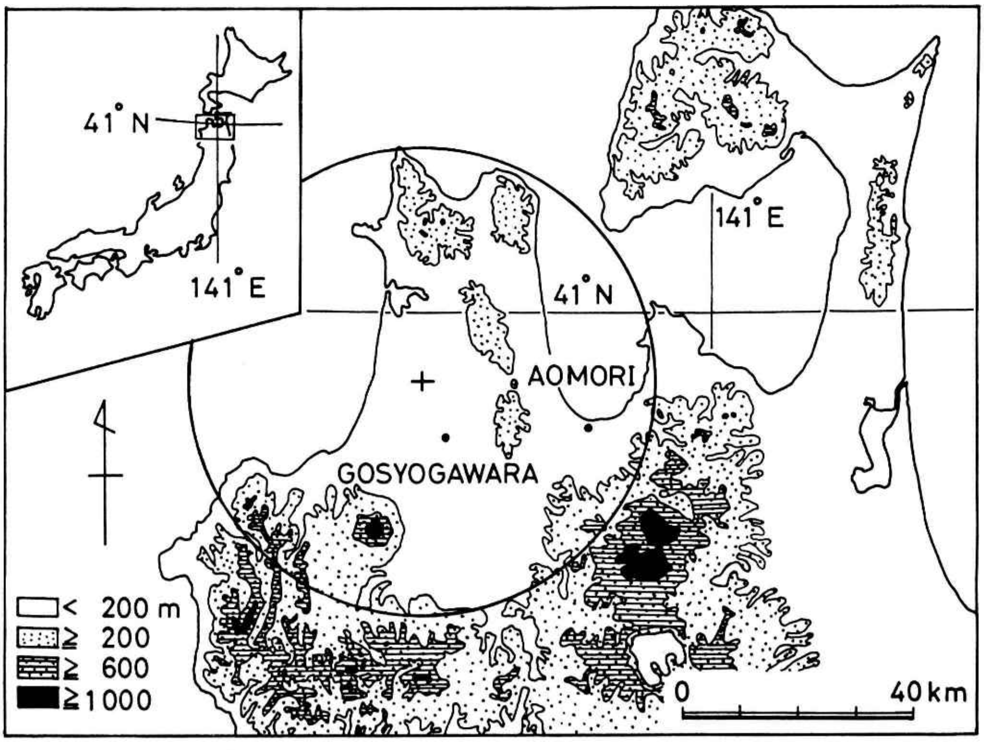


**Fig. 10** Schematic map showing the topography in and around the observation ares and the location of the Doppler radar, Tsugaru, 1989. The cross mark shows the location of the radar and the circle shows the radar observation range.

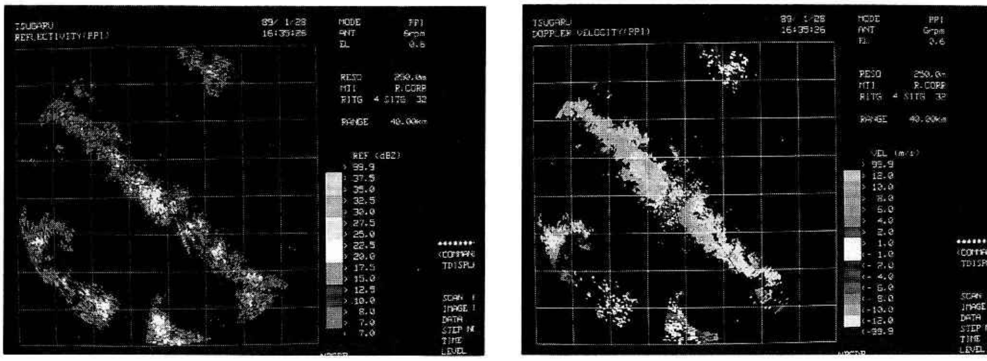


**Fig. 11** PPI display of (a) the reflectivity factor, (b) Doppler velocities for the snowstorm of January 28, 1989 in the Tsugaru plain.

height. To overcome this restriction and carry out a more extensive observation of this type of snowstorm, the use of the Doppler radar was proposed. A comprehensive study using a Doppler radar, radiosonde measurements, and surface layer measurements began in January of 1989. Fig. 10 shows the observation area and the location of the Doppler radar. The purpose of the Doppler radar observation is to clarify the area and the duration time of the snowstorm and to develop a method predicting the occurrence of the storm.

One example of the snowstorms observed with the Doppler radar is shown in the PPI display in Fig. 11. The storm formed over the Japan Sea under a strong winter monsoon burst and drifted eastward. The band-shaped snowstorm in Fig. 11(a) passed over the radar site, which is the center of the picture, and it dissipated over the Tsugaru Peninsula after about one hour. The storm was associated with the strong wind shown in the PPI display of Doppler velocities in Fig. 11(b). Because the elevation angle is small (0.6 degree), the pattern of Doppler velocities gives information about the wind field near the surface. It can be seen that the wind direction was from the northwest to the sontheast and the maximum wind speed was over 20 m/s.

*OROGRAPHICALLY ENHANCED SNOWFALL*

The research project for investigating the actual conditions of snow clounds over the Japan Sea in the winter and studying the possibility of artificial snowfall control was started in February, 1989. The NRCDP participated in the research program and observed snowfall in the inland areas in the Tohoku District of Japan. The main purpose of the program was to clarify the effect of topography on snowfall and to give the basic information about the change of snowfall under natural conditions when a quantitative estimation of artificial control of snowfall is required. A schematic map showing the topography in and around the observation area and the locations of the Doppler radars are shown in Fig. 12. Three Doppler radars were used in the project. Doppler radars from the Institute of Low Temperature Science (ILTS) of Hokkaido University and the NRCDP were arranged to observe the change in the snow clouds over the Dewa hills,

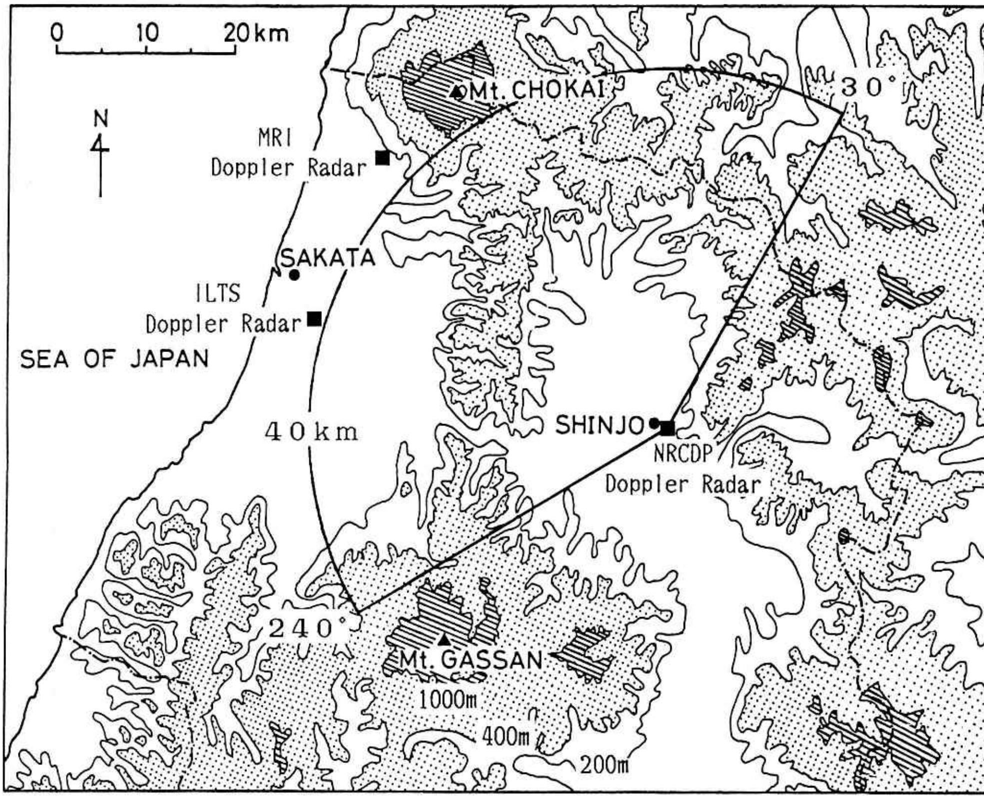


**Fig. 12** Schematic map showing the topography in and around the observation area and the location of the Doppler radar, Shinjo, 1989.

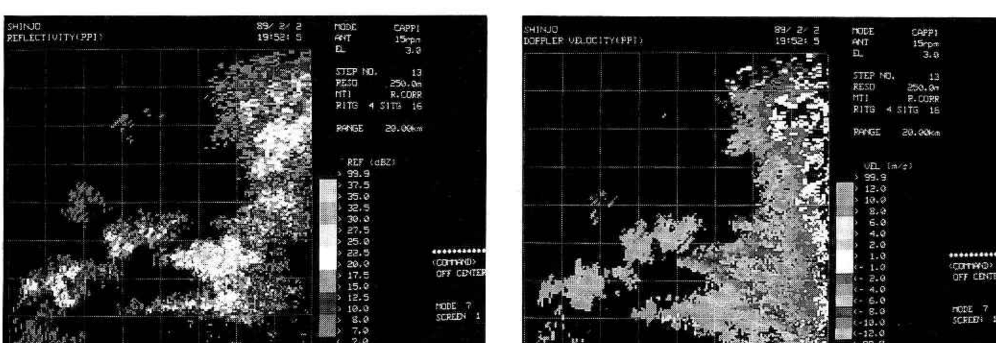


**Fig. 13** PPI display of (a) the reflectivity factor, (b) Doppler velocities for the orographically enhanced snowfall of February 2, 1989 in the Shinjo Basin.

located between two radars, while the radars of ILTS and MRI (Meteorological Research Institute) of JMA were used to observe the snow clouds over the Sea of Japan by dual measuring modes.

One example of orographically enhanced snow which was observed February 2, 1989 is shown in Fig. 13. The location of the radar is in the lower right hand corner of the rectangle and the grid interval is 5 km. The PPI picture of the radar reflectivity factor (Fig. 13(a)) shows a topographically enhanced snowfall echo about 20 km northwest of the radar site. This area is over the east side of the Dewa hills and corresponds to the downind slopes of the hills. It is also interesting to note that there is a strange pattern of the Doppler velocity in the area which corresponds to the area of the enhanced snowfall (Fig. 13(b)).

## 4. Concluding remarks

The Doppler radar of the National Research Center for Disaster Prevention was completed in March, 1988. The main characteristics of the radar are rapid scanning of the radar antenna and various scan modes controlled by a computer. These performances are useful to observe severe weather phenomena whose horizontal scales are small and lifetimes are short.

The antenna scan mode, which is appropriate to observe a weather phenomenon three-dimensionally, depends on the horizontal and vertical dimension of the pheno-

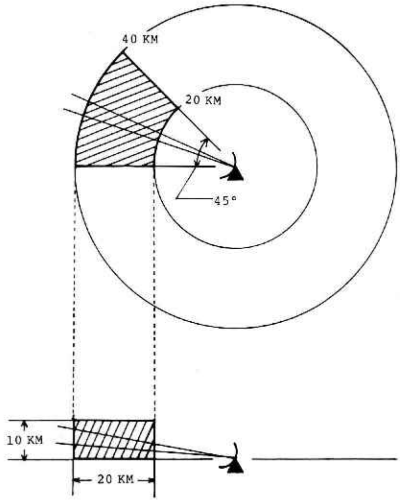


| SCAN MODE | SPEED | OBSERVATION TIME |
|---|---|---|
| CAPPI | 90 deg/sec (15rpm) | ~4' 40" |
| SPPI | 18 deg/sec | ~4' 50" |
| SRHI | 18 deg/sec | ~4' 10" |

**Fig. 14** Schematic pictures of vertically extended phenomena and observation time of various scan modes requied for the three-dimensional measurement of the phenomena.

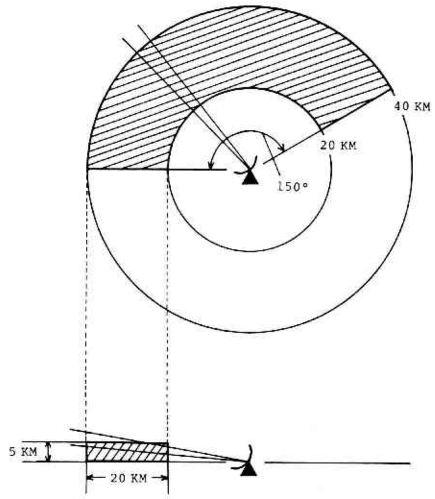


| SCAN MODE | SPEED | OBSERVATION TIME |
|---|---|---|
| CAPPI | 90 deg/sec (15rpm) | ~ 2' 40" |
| SPPI | 18 deg/sec | ~ 4' 0" |
| SRHI | 18 deg/sec | ~10' 50" |

**Fig. 15** As in Fig. 14 except for horizontally extended phenomena.

menon. Two cases of the phenomena were considered; one is a phenomenon which extens vertically but with a small horizontal scale (Fig. 14) and the other is a phenomenon which extends horizontally but with a shallow depth (Fig. 15). A typical example of the former case is a convective storm and that of the latter case is the precipitation from a stratiform cloud or snowfall in the Tohoku District in winter. The observation time required for a three-dimensional scan of the phenomena is calculated and listed in the tables in Fig. 14 and Fig. 15 for CAPPI, SPPI and SRHI scan modes. It can be seen that the CAPPI scan mode is the most suitable antenna operation mode for the observation of horizontally extended phenomena. On the other hand, these three modes can hardly be compared in the case of vertically extended phenomena as far as observation time is considered. However, considering the amount of data, the SPPI or SRHI mode may be the suitable scan mode.

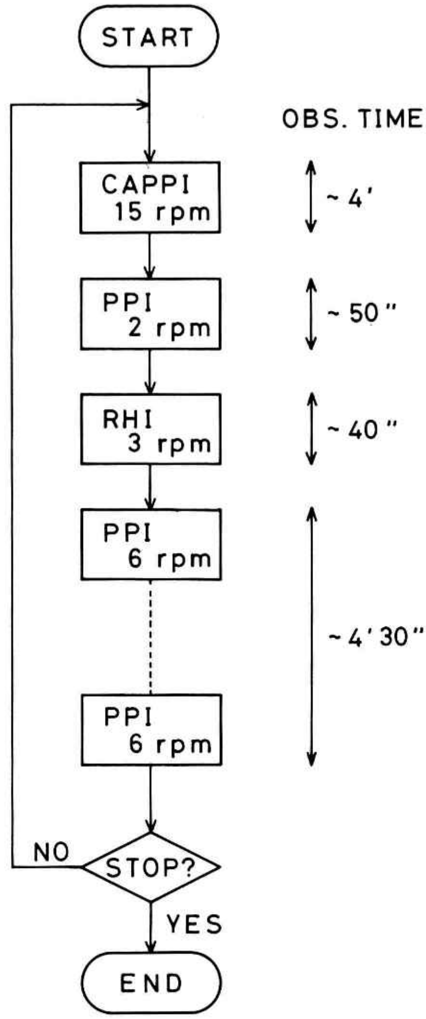


**Fig. 16** Flow chart of antenna scan modes used in snowstorm observations at Tsugaru.

In the observation of the snowstorms at the Tsugaru plain, a set of antenna scan modes shown in Fig. 16 was planned and used. The first scan mode, CAPPI, which consists of 19 PPI modes (elevation angle from 0 to 20.4 degrees), is for three-dimensional data acquisition of the snowstorms. The second mode, PPI (the elevation angle is 20 degrees), is for VAD (Velocity Azimuth Display) and used to obtain the vertical wind profile at the radar site. The third mode, RHI, is for the observation of the vertical structure of the snowstorm. The azimuth angle was usually set to the wind direction. The remaining PPI modes (the elevation angle is 0.6 degrees) are for the monitoring of the occurrence and movement of the snowstorm. Observation times required for CAPPI (15rpm), PPI (2rpm), PHI (3rpm) are about 4 minutes, 50 seconds, and 40 seconds, respectively. The period of the monitoring mode (PPI modes) is about 4 minutes and 30 seconds, and the total observation time for a set of scan modes shown in Fig. 16 is about 10 minutes.

The thunderstorm observed in summer of 1988 is a good example which shows the effectiveness of NRCDP's Doppler radar. The radar could detect a thunderstorm which could not be observed by present observation systems such as that of AMeDAS. Unfortunately, because the observation was carried out during an efficiency test of the radar, the whole stage of the thunderstorm development could not be clarified. Two examples of radar observations in winter are also given in this paper. One is a snowstorm accompanied with strong wind and the other is snowfall enhanced by the topography. Analyses are now in progress and examples shown in this paper are only preliminary results of the analyses.

**Acknowledgments**

The authors wish to thank Inagaki Village, Gosyogawara City of Aomori Prefecture, Shinjo City of Yamagata Prefecture, and the Shinjo branch of NRCDP for providing all accommodations for radar observation. The research on the topographically enhanced snowfall was supported by Special Coordination Funds for Promoting Science and Technology of the Science and Technology Agency of Japan.

## References

1) Browning, K. A. (1982): *Now casting*, Academic press, 256 pp.
2) Kinosita T., T. Mizutani, T. Yagi, T. Kishii, T. Sato, S. Uehara, H. Ohkura and S. Kishi (1987): *Investigation of major natural disasters, No. 27*, National Research Center for Disaster Prevention, Japan, 155 pp.
3) Maki, M. (1989): Effect of rapid scan of the Doppler radar on the estimation of spectrum moments. *Rep. National Research Center for Disaster Prevention*, **44**, 81-94.
4) Oyagi, N., K. Nakane and T. Fukuzono (1984): *Investigation of major natural disasters, No. 21*, National Research Center for Disaster Prevention, Japan, 133 pp.
5) Sato, A. and M. Higashiura (1989): Effect of air temperature and wind speed on occurrence of blowing snow. *Rep. National Research Center for Disaster Prevention*,**43**, 255-262.
6) Tanaka, T., S. Nakai and K. Nakane (1988): *Investigation of major natural disasters No. 30*, National Research Center for Disaster Prevention, Japan, 115 pp.
7) Uyeda, H. (1986): On recent observations and detections of storms by Doppler radar for meteorological use. *Review of R.D.P., No. 111*, National Research Center for Disaster Prevention, Japan, 61 pp.
8) Vincent, T. W. and R. A. Brown (1985): Single Doppler velocity signature interpretation of nondivergent environmental winds. *J. Atmos. Oceanic Technol.*, **3**, 114-128.

(Manuscript Received July 24, 1989)

# 国立防災センターのドップラーレーダーの特徴とメソスケールの大気現象の観測について

真木雅之*・八木鶴平*・中井専人*

国立防災科学技術センター

## 要旨

メソスケールの大気現象を研究するためのドップラーレーダーが1988年3月に完成した．本ドップラーレーダーの主な特徴として

1) 様々な空中線スキャンモードを有し，コンピュータにより制御される．
2) 空中線の高速回転（最大15 rpm）．
3) レーダー反射強度，ドップラー速度，ドップラースペクトル幅のオンラインカラー表示．
4) 可搬型．

が挙げられる．本ドップラーレーダーによる観測例として梅雨期の層状性降水，夏期の雷雨，津軽平野での吹雪，新庄での地形により強化された降雪現象を紹介し，最後に現象の3次元的な観測のための空中線最適スキャンモードについて議論した．

* 第1研究部，広域防災研究室